

Low-Coherence Interferometric Measurements of the Dispersion of Multiple Fiber Bragg Gratings

Shellee D. Dyer, *Member, IEEE* and Kent B. Rochford, *Member, IEEE*

Abstract—We show that the dispersion of multiple fiber Bragg gratings can be obtained from a single low-coherence interferometric measurement. The individual gratings can be identified either from the spatial separation of the interferometric signatures or from the unique wavelength-reflection bands of the gratings.

Index Terms—Chromatic dispersion, fiber Bragg grating, group delay, interferometry, optical fibers, white light.

I. INTRODUCTION

LOW-COHERENCE interferometry has several advantages over conventional techniques for the characterization of fiber Bragg gratings (FBGs). A key advantage is the rapidity with which the group delay can be obtained. The interferogram is obtained in less than a second, and processing the interferogram to obtain the group delay takes less than 60 seconds [1], compared with the modulation phase-shift measurement, which can take several hours [2].

Rapid group delay measurements have also been demonstrated using a frequency-domain method [3]. That technique uses a tunable laser diode rather than a broad-band source, and the measured signal is a function of wavelength, rather than optical path difference (OPD). The frequency-domain technique requires two Fourier transforms to calculate the group delay, compared to only one for the low-coherence method.

The low-coherence technique has good repeatability (better than 1 ps) and, because of its speed, is immune to errors caused by thermal variations and instrument drift. Low-coherence interferometry is also immune to the type of ripple washout problems that can occur with the modulation phase-shift measurement [4].

In this letter, we demonstrate the measurement of the group delay of individual FBGs in cascaded assemblies. This is important in telecommunications applications where several gratings are used in series as add/drop multiplexers [5], and in cases where several gratings are concatenated to achieve desired dispersion characteristics [6].

II. MEASUREMENT METHOD

A diagram of the low-coherence interferometric system is shown in Fig. 1. A broad-band erbium (Er) superfluorescent

fiber source (SFS) provides the input signal. Fiber coupler 1 provides a comparison signal for the difference-over-sum (Δ/Σ) amplifier, as explained below. Fiber coupler 2 is part of a Michelson interferometer. Three FBGs are spliced onto the test arm of the interferometer. FBGs A and C have overlapping reflection bands; therefore, fiber coupler 3 separates these two gratings to eliminate Fabry-Perot and shadowing effects.

The reference arm of the interferometer contains a variable-length air path so that the total OPD of the interferometer can be varied. A frequency-stabilized HeNe-laser interferometer monitors the position of the reference-arm mirror, and a zero-crossing detector triggers sampling of the IR signal on positive-sloped zero crossings of the HeNe signal. A polarization controller is used to optimize the fringe visibility by matching the polarization state of the reference arm signal to that of the test arm.

The light from the reference arm is recombined with the light from the test arm at fiber coupler 2, and the recombined light is directed onto the two IR detectors. The detected signals have similar source excess-noise characteristics, while the interference terms are 180° out of phase due to coupler 2. Therefore, using a Δ/Σ amplifier will reduce excess noise from the SFS, which is the dominant noise source. This improves the interferogram's signal-to-noise ratio (SNR) by a factor of 3, and yields a corresponding improvement in the group-delay SNR.

If the effective spatial separation between the FBGs exceeds the width of the individual coherence functions, then the output signal of the Δ/Σ amplifier, as a function of OPD, consists of three distinct signatures. Each of these signatures represents the interference of light reflected from one of the FBGs with light reflected from the reference-arm mirror.

The shape and extent of the interferometric signatures from FBGs A and C are determined by their reflection characteristics. The output $V(\xi)$ of the Δ/Σ amplifier for either of these signatures is given by [7]

$$V(\xi) \propto \text{Re} \left\{ \int_{-\infty}^{\infty} G(\sigma) r(\sigma) \exp(j\phi_r(\sigma)) \exp(j2\pi\sigma\xi) d\sigma \right\} \quad (1)$$

where ξ is the OPD, σ is the wavenumber, $G(\sigma)$ is the power spectral density of the Er SFS, and $r(\sigma)\exp(j\phi_r(\sigma))$ is the complex field reflection coefficient of the corresponding FBG. The reflection group delay (t_g) of each grating is calculated from the phase of the Fourier transform of $V(\xi)$ as follows:

$$t_g = \frac{1}{2\pi c} \frac{d}{d\sigma} \phi_r(\sigma). \quad (2)$$

Manuscript received August 22, 2000; revised November 6, 2000.

S. D. Dyer is with the National Institute of Standards and Technology, Optoelectronics Division, Boulder, CO 80305 USA (e-mail: sdyer@boulder.nist.gov).

K. B. Rochford was with the National Institute of Standards and Technology, Optoelectronics Division, Boulder, CO 80305 USA. He is now with Yafo Networks, Inc., Hanover, MD 21076 USA.

Publisher Item Identifier S 1041-1135(01)01994-2.

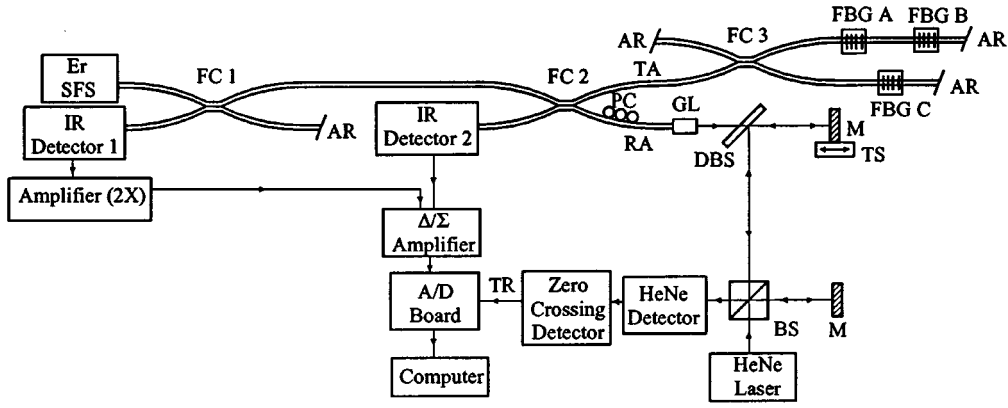


Fig. 1. Diagram of low-coherence interferometric system for measuring the dispersion of multiple FBGs. AR: antireflection coating, FC: fiber coupler, RA: reference arm, TA: test arm, PC: polarization controller, GL: grin lens, M: mirror, TS: translation stage, BS: beamsplitter, DBS: dichroic beamsplitter, Δ/Σ : difference over sum.

The light transmitted by grating A and reflected by grating B sees the effects of both gratings A and B, and the output of the Δ/Σ amplifier for this interferometric signature is related to both gratings as follows:

$$V(\xi) \propto \text{Re} \left\{ \int_{-\infty}^{\infty} G(\sigma) [t_A(\sigma) \exp(j\phi_{t_A}(\sigma))]^2 r_B(\sigma) \cdot \exp(j\phi_{r_B}(\sigma)) \exp(j2\pi\sigma\xi) d\sigma \right\} \quad (3)$$

where $t_A(\sigma) \exp(j\phi_{t_A}(\sigma))$ is the complex field transmission coefficient of grating A, and $r_B(\sigma) \exp(j\phi_{r_B}(\sigma))$ is the complex field reflection coefficient of grating B. The equations above were derived assuming that the only difference in group delay between the two arms arises from the group delay of the FBGs. In reality, there is a small background group delay arising from the difference in the length of the test and reference arm fibers, but it is negligible compared with the group delay of a typical FBG [8].

It is also possible to measure the transmission group delay of a single grating using a variation of the system shown in Fig. 1. We replaced fiber coupler 3 and the three gratings with grating A spliced directly to the test arm of fiber coupler 2. We cleaved the far end of grating A's fiber pigtail to produce a Fresnel reflection. In this case, the interferogram consists of a pair of signatures. The first signature represents the interference of light reflected by grating A with light from the reference arm, as given by (1). The second signature represents the interference of light reflected by the cleaved endface with the light from the reference arm. This signature is related to FBG A's transmission function as follows:

$$V(\xi) \propto \text{Re} \left\{ \int_{-\infty}^{\infty} G(\sigma) [t_A(\sigma) \exp(j\phi_{t_A}(\sigma))]^2 \cdot \exp(j2\pi\sigma\xi) d\sigma \right\} \quad (4)$$

where $t_A(\sigma) \exp(j\phi_{t_A}(\sigma))$ is the complex field transmission coefficient of FBG A.

III. DATA PROCESSING

There are two options for processing a multigrating interferogram to obtain group delay. One option (method #1) is to separate the interferogram array into three separate arrays, each centered on an individual FBG signature. Each FBG signature is truncated near the points where the SNR is approximately unity. Next, we append zeros to each array (zero padding) to obtain three arrays, each of length 2^N . The choice of N determines the wavelength resolution of the group delay results. Larger values of N give better resolution, but if N is too large, computational errors such as roundoff error will affect the accuracy of the results. For the results shown in this letter, we use $N = 18$, giving a wavelength resolution of 14 pm. To obtain the group delay, we take the Fourier transforms of each truncated and padded interferogram. The relative group delay of the FBG is determined by differentiating the phase of the corresponding Fourier transform. This processing option can be applied only in cases where the interferometric signatures do not overlap.

Another processing option (method #2) involves calculating the group delay of all three gratings simultaneously, by calculating a Fourier transform of the entire interferogram. If the reflection bands of the three gratings do not overlap, then the group delay of each individual grating can be identified as a function of wavelength. The problem that arises in simultaneously processing multiple signatures is that the separation between the signatures leads to a sinusoidal beating function in the Fourier transform. The period of this sinusoidal function is determined by the spatial separation between the gratings; in cases where the separation is small, the period of this sinusoidal function is large enough to be neglected. In cases involving large separation between gratings, we eliminate this sinusoidal function by truncating each grating's signature near the unity SNR points. Next, we calculate the central fringe of each interferogram [9], and we shift the individual arrays such that the three central fringes are all at the same point. Then we add the three interferogram arrays, zero pad the total array to a length of 2^N , and calculate the Fourier transform. We obtain the group delay by differentiating the phase of the Fourier transform, and identify each individual grating from its respective wavelength reflection band. This processing technique can be applied to cases in which the interferometric signatures of the gratings spatially overlap, as long as their respective wavelength reflection bands are nonoverlapping.

TABLE I
SPECIFICATIONS OF THE THREE GRATINGS

Grating	Center Wavelength (nm)	Reflection Bandwidth, FWHM (nm)	Reflectance (%)
A	1555.6	5.4	99
B	1541.3	10.1	>97
C	1554.7	1.7	>99

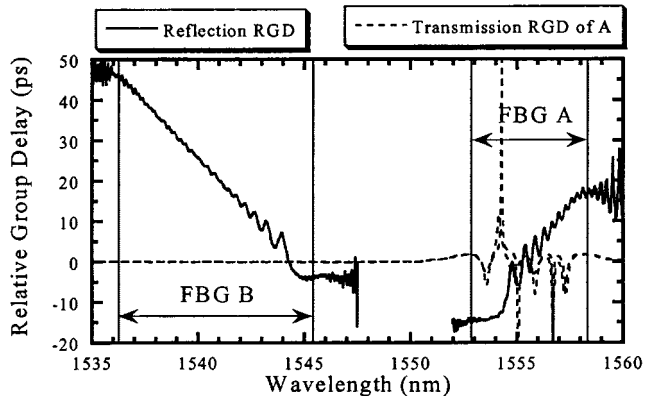


Fig. 2. Relative group delay (RGD) of gratings A and B calculated individually using processing method #1. Also shown is the transmission RGD of grating A. To illustrate the measurement's repeatability, results are shown from two separate measurements. The relative group-delay difference due to the fiber delay between the two gratings is not shown.

IV. EXPERIMENTAL RESULTS

We used our interferometric system to determine the reflection group delay of three gratings. The center wavelengths, reflection bandwidths, and reflectances of the three gratings are shown in Table I. Gratings A and B were separated by approximately 7 cm of fiber, and the effective fiber separation between gratings A and C was 8 mm. The interferogram in this case consisted of three distinct signatures created by interference of the reflections from each of the three gratings with light from the reference arm.

We calculated the group delay of each of the three gratings using processing method #1. The group delay results for gratings A and B are shown in Fig. 2. For grating A, this group delay is simply the relative reflection group delay of the grating. In the case of grating B's interferometric signature, the group delay is a product of the reflection group delay of B with twice the transmission group delay of grating A, as given by (3). The double-pass transmission group delay of grating A is also shown in Fig. 2. From this graph it is clear that the transmission-group delay of grating A is very small in the reflection band of B, and therefore it can be neglected compared with the reflection-group delay of grating B.

We also calculated the group delays using processing method #2. Since gratings A and C have overlapping reflection bands, their group delays cannot be separated in wavelength, and processing method #1 above is the only way to calculate the group delay of these two gratings. However, it is possible to simultaneously calculate the group delay of gratings A and B or B and C

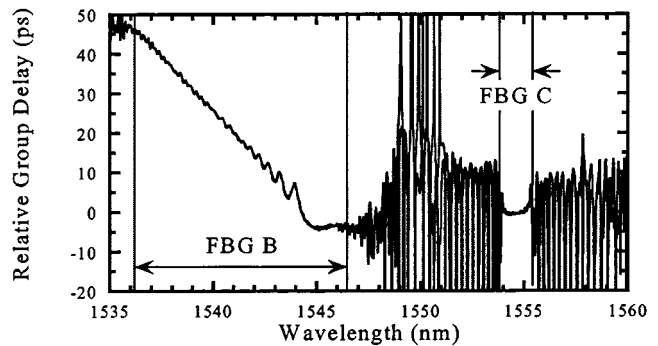


Fig. 3. Relative group delay of gratings B and C calculated simultaneously using processing method #2. Results are shown from two repeated measurements. The relative group-delay difference due to fiber delay between the two gratings is not shown.

using method #2. Simultaneously calculating the group delay of gratings B and C gives the results shown in Fig. 3. We identified the group delay of gratings B and C from their known reflection bands, also shown in Fig. 3.

V. CONCLUSION

We have demonstrated a high-speed measurement of the group delay of multiple cascaded gratings using low-coherence interferometry. We have shown that the group delay of individual gratings in series can be determined regardless of overlapping reflection bands. This is an important advantage of the low-coherence technique; the modulation-phase shift measurement is incapable of distinguishing between individual components with overlapping reflection bands.

REFERENCES

- [1] S. D. Dyer, K. B. Rochford, and A. H. Rose, "Fast and accurate low-coherence interferometric measurements of fiber Bragg grating dispersion and reflectance," *Opt. Exp.*, vol. 5, pp. 262–266, Nov. 1999.
- [2] S. E. Mechels, J. B. Schlager, and D. L. Franzen, "Accurate measurements of the zero-dispersion wavelength in optical fibers," *J. Res. Natl. Inst. Stand. Technol.*, vol. 102, pp. 333–347, May/June 1997.
- [3] M. Froggatt, T. Erdogan, and J. Moore, "Optical frequency domain characterization of dispersion in optical fiber Bragg gratings," in *Bragg Gratings, Photosensitivity, and Poling in Glass Waveguides*, OSA Tech. Dig., Stuart, FL, 1999, pp. 227–229.
- [4] R. M. Fortenberry, "Enhanced wavelength resolution chromatic dispersion measurements using fixed sideband technique," in *Optical Fiber Communications Conf., OSA Tech. Dig.*, Baltimore, MD, 2000, pp. 107–109.
- [5] B. J. Eggleton, G. Lenz, N. Litchinitser, D. B. Patterson, and R. E. Slusher, "Implications of fiber grating dispersion for WDM communication systems," *IEEE Photon. Technol. Lett.*, vol. 9, pp. 1403–1405, Oct. 1997.
- [6] L. D. Garrett, A. H. Gnauck, R. W. Tkach, B. Agogliati, L. Arcangeli, D. Scarano, V. Gusmeroli, C. Tosetti, G. Di Maio, and F. Forghieri, "Cascaded chirped fiber gratings for 18-nm-bandwidth dispersion compensation," *IEEE Photon. Technol. Lett.*, vol. 12, pp. 356–358, Mar. 2000.
- [7] U. Wiedmann, P. Gallion, and G.-H. Duan, "A generalized approach to optical low-coherence reflectometry including spectral filtering effects," *J. Lightwave Technol.*, vol. 16, pp. 1343–1347, July 1998.
- [8] S. D. Dyer and K. B. Rochford, "Low-coherence interferometric measurements of fiber Bragg grating dispersion," *Electron. Lett.*, vol. 35, pp. 1485–1486, Aug. 1999.
- [9] B. L. Danielson and C. Y. Boisrobert, "Absolute optical ranging using low-coherence interferometry," *Appl. Opt.*, vol. 30, pp. 2975–2979, July 1991.